Fluid Phase Equilibria 402 (2015) 30–37

Contents lists available at ScienceDirect

Fluid Phase Equilibria

journal homepage: www.elsevier.com/locate/fluid

Stability and cell distortion of sI clathrate hydrates of methane and carbon dioxide: A 2D lattice-gas model study

P. Longone [a,*], A. Martín [b], A.J. Ramirez-Pastor [a]

[a] Departamento de Física, Instituto de Física Aplicada (INFAP), Universidad Nacional de San Luis, CONICET, Ejército de los Andes 950, D5700HHW San Luis, Argentina

[b] Departamento de Ingeniería Química y Tecnología del Medio Ambiente, Facultad de Ciencias, Universidad de Valladolid, 47011 Valladolid, Spain

ARTICLE INFO

Article history:
Received 23 February 2015
Received in revised form 18 May 2015
Accepted 20 May 2015
Available online xxx

Keywords:
Clathrate hydrates
Lattice-gas model
Monte Carlo simulations
Methane
Carbon dioxide

ABSTRACT

Thermodynamic models of the stability of clathrate hydrates are important for different applications such as the storage, separation and transport of gases. The development of improved models relies on a better understanding of the relationships between the macroscopic stability of clathrate hydrates and their structure. In particular, lattice distortion is an important parameter that is difficult to incorporate in thermodynamic models of clathrate hydrates. In this work, a 2D lattice-gas model has been applied for the first time for the study of the stability and lattice distortion of sI clathrate hydrates of methane and carbon dioxide. Results show a direct relationship between cell distortion and cell occupancy: the minimum distortion is found at cell occupancies near 1. In addition, in the case of carbon dioxide hydrates, a complex behavior is observed due to the partial occupancy of small cavities by guest CO_2 molecules. By relating lattice distortion with hydrate stability, phase diagrams can be calculated which are in qualitative agreement with experimental diagrams and with results of more complex simulation methods.

1. Introduction

Clathrate hydrates are solid cage structures formed by mixtures of water and low molecular weight components that belong to a class of compounds called inclusion clathrates [1,2]. In these compounds, water molecules form a regular crystal lattice, which gives rise to the formation of cavities where guest (host) molecules can be adsorbed. Hydrogen bonds between water molecules can lead to various types of cavities, with specific sizes and geometries: pentagonal dodecahedron (5^{12}), tetrakaidecahedron ($5^{12}6^2$), hexakaidecahedron ($5^{12}6^4$), irregular dodeca-hedron ($4^3 5^6 6^3$), and icosahedrons ($5^{12}6^8$). Symbols between parentheses correspond to Jeffrey's notation of these cavities [3,4]. The combination of different number and type of cavities build up unit cells. Then, a set of unit cells form the gas hydrate structures: sI, sII and sH [1,2]. Of these, the most commonly observed hydrate structures are sI and sII. They consist of tetrakaidecahedral ($5^{12}6^2$) and hexakaidecahedral ($5^{12}6^4$) clusters, 12 pentagonal with 2 hexagonal rings of water molecules (24 water molecules) and 12 pentagonal with 4 hexagonal rings of water molecules (28 water molecules), respectively. The structure and stability of the regular crystal lattice depend on the nature, size and shape of the guest molecules that occupy the cavities. Gas molecules such as methane, ethane and carbon dioxide form type sI hydrates, while larger molecules preferably form sII (propane, iso-butane) and sH (cyclohexane, cycloheptane) structures.

In the last years, high amounts of methane in hydrate deposits have been found. Natural geologic environments such as depths in the oceans and arctic permafrost regions are huge deposits of methane hydrates. These large quantities of methane represent a powerful new source of energy for the future [5–7]. It has also been estimated that there are more energy resources in these hydrates than in fossil fuels [8,9]. Because of the large amounts of methane available in these reserves, the study of methane hydrates have attracted the researchers' attention. In addition, CO_2 hydrates have also been known for years [10]. These hydrates are often thought as agents for global climate change and they have received attention from a large group of scientists [1,11,12]. Besides, it has been hypothesized that the release of greenhouse gases from the natural clathrates played a role in past climate changes [13]. The amount of carbon stored in natural carbon dioxide clathrates is about twice the organic carbon present in fossil fuels [14]. Therefore, the development of technologies for the exploitation of this resource is of great interest.

Clathrate hydrates have different technological applications such as separation, storage and transport of gases [15]. Nowadays,

* Corresponding author. Tel.: +54 26644520329.
E-mail address: plongone@unsl.edu.ar (P. Longone).

http://dx.doi.org/10.1016/j.fluid.2015.05.035
0378-3812/

there is a limited amount of experimental data about the properties, composition and formation conditions of clathrate hydrates, and quantity of gas stored. Due to these reasons, detailed and precise thermodynamic models have been developed to predict the phase behavior of clathrate hydrates. van der Waals and Platteeuw (vdWP) [16] theory was developed in 1958, by combining mechanical statistics with classical theory of adsorption (Langmuir model). In this theory, it is assumed that the interactions between guest molecules and the aqueous lattice are relatively weak and they are limited to the nearest neighbors (NN) of the gas molecule. Besides, the interactions between host molecules corresponding to different cavities are neglected, and multiple occupancy of the cavities by several gas guest molecules is not considered. Therefore, the behavior of each guest molecule does not depend on the presence of other guest molecules. Later this classic model was widely studied for Parrish and Prausnitz [17] for multicomponent gas hydrates. The authors introduced some modifications on the theory vdWP [18–20]. The modifications are related to the phenomenon of flexibility of the hydrogen-bonded and multiple occupation of cavities. However, original vdWP theory still continues to be the more important and widely-used theoretical tool for gas hydrate research.

In the last years, computational simulations have proved to be a useful tool for studying the degree of occupation and predicting the stability of the cavities that form the clathrate hydrates [21–30]. The importance of computer simulations has been tested by different authors through the comparison with experiments and theoretical predictions [31,32]. Pimpalgaonkar et. al calculated the triple-point lines of methane and ethane by using Monte Carlo (MC) simulations [31]. Papadimitriou et al. reported the number of occupied cavities for He and THF [32]. The results show that large cavities are completely occupied by THF molecules, whereas the small ones are partially occupied by He atoms.

On the other hand, it is well known that there are effects of lattice distortion in hydrates when the cavities are occupied with guest species of different sizes. An important contribution to this subject was made by Zele et al. [24]. The authors showed that large guest molecules lead to a deformation of the hydrate lattice, known as lattice expansion. This expansion causes an increase in the difference between the chemical potential of water in the empty and filled lattice. Simulations of cell volume as a function of guest size showed an increase in the cell volume with increasing guest parameters [33]. In the same way, Martín and Peters [34] developed a new thermodynamic theoretical model considering lattice distortion by introducing a distortion model of the chemical potential for vdWP [16]. The authors found an increase in the distortion of the chemical potential with increase in the size of the host species. In 2007, Sizov and Piotrovskaya [26] studied the behavior of occupancy isotherms for flexible and rigid methane hydrate through grand canonical MC simulations (using a three-dimensional (3D) algorithm). Simulations were carried out using the SPC/E model for water [35] and UA model for methane molecules [36]. The system used contained eight ($2 \times 2 \times 2$) sI methane hydrate unit cells with 3D periodic boundary conditions.

Even though many aspects of the problem have been studied, other points still remain open. Namely, (i) all works mentioned above [21–30] require a big number of parameters, and (ii) there is a lack of models able to predict the degree of deformation and its relation to the stability of clathrate hydrates. Here, we attempt to remedy this situation. Accordingly, the main objectives of the present paper are (1) to develop a simple lattice-gas model capable to describe the behavior of clathrate hydrates, reducing the number of parameters; (2) to study the degree of deformation of gas hydrates in the presence of CO_2 and CH_4 species; and (3) to predict the conditions in which the hydrate is more stable. This work is limited to the structure sI and methane and carbon dioxide host species. These host species have important implications as new energy sources.

Lattice-gas model has proved to be useful for the description of a wide variety of phenomena in physics and beyond [37]. During the early part of the past century, two important methods of investigation of lattice-gas model were developed: the Bragg–Williams approximation [38] and the quasichemical approximation [38]. More recently, substantial progress has been made in the development of accurate and powerful approximations as real-space renormalization-group technique [39], transfer-matrix method [40] and finite-size scaling theory [41]. As result of these investigations, the lattice-gas theory, initially proposed to model a ferromagnet [42–44], is today one of the most active research areas in the treatment of phase transitions and critical phenomena [37].

In the case studied here, the application of the lattice-gas model, as well as the reduction of the system to 2D, is not only of academic interest but important for understanding the phenomenon of cavity distortion as a result of the presence of guest species. This study is a first step towards a more accurate determination of the phase behavior of the system, which will be the object of future research.

2. Lattice-gas model and Monte Carlo simulation scheme

2.1. Lattice-gas model: sI hydrate structure

In this section, the distortion of the structure of sI gas hydrates in the presence of CO_2 and CH_4 is modeled by using a 2D lattice-gas

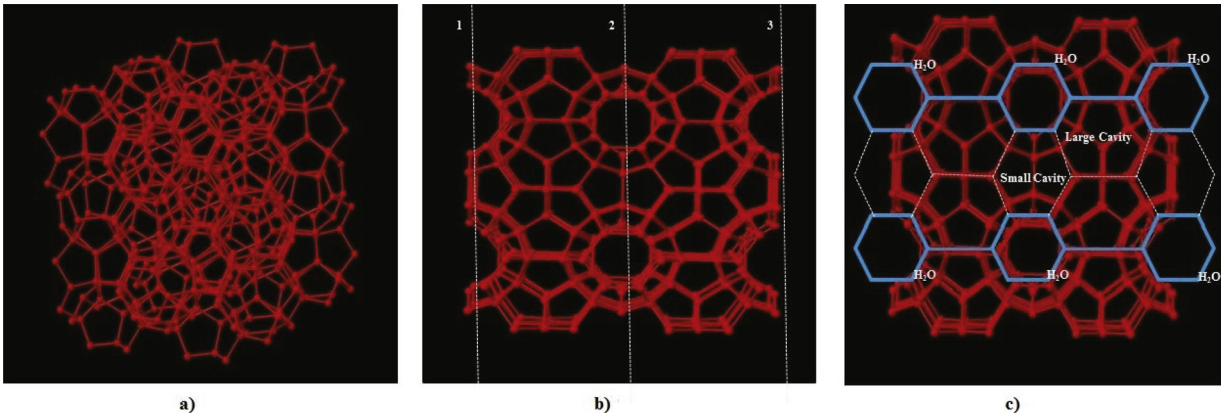

Fig. 1. (a) Scheme of the 3D structure of a portion of sI clathrate hydrate composed by eight ($2 \times 2 \times 2$) unit cells. (b) Part (b) is a view observing the structure of part (a) in one direction along either the *x*,*y* or *z* axis. (c) Identification of water molecules that form the hexagons which build up the structure sI in 2D.

model and Monte Carlo simulations. A similar scheme has been previously used to study adsorption and diffusion of polyatomic species on homogeneous surfaces [45–50]. Making an analogy with adsorption–desorption process, the gas hydrate is considered as a lattice of sites with a specified geometry. In addition, the stability of hydrate is assumed explicitly before simulation [21–30].

Let us consider a portion of sI clathrate hydrate, which is composed by eight ($2 \times 2 \times 2$) unit cells, see Fig. 1a [51]. Each unit cell contains two dodecahedron cavities (5^{12}) (small cavity) and six tetrakaidecahedron cavities ($5^{12}6^2$) (large cavity). The 3D points correspond to water molecules. For simplicity, only the oxygen atoms of water are shown in Fig. 1a.

Fig. 1b is a view observing the structure of Fig. 1a along the direction of *x*, *y* or *z* axis. By cutting the structure of sI clathrate hydrate with a plane parallel to the *xz* plane and passing through the center of the structure [line 2 in Fig. 1b], one obtains two equivalent faces. The same result can be obtained by cutting the structure in part b, with planes passing through the lines 1 and 3. Thus, the structure sI has symmetry in faces 1–3. This property allows us (1) to reduce the 3D sI structure to a set of 2D planes as shown in Fig. 1c and (2) to study the behavior of clathrate hydrates in the presence of guest species, through an analogy with the adsorption–diffusion process in a 2D lattice-gas model with multiple occupation of sites [45–50].

From the scheme in Fig. 1c, hexagons formed by the oxygen atoms of the water molecules can be identified. These hexagons correspond to the top of the cavities. In addition, empty spaces can be linked to large and small cavities (represented by dotted lines).

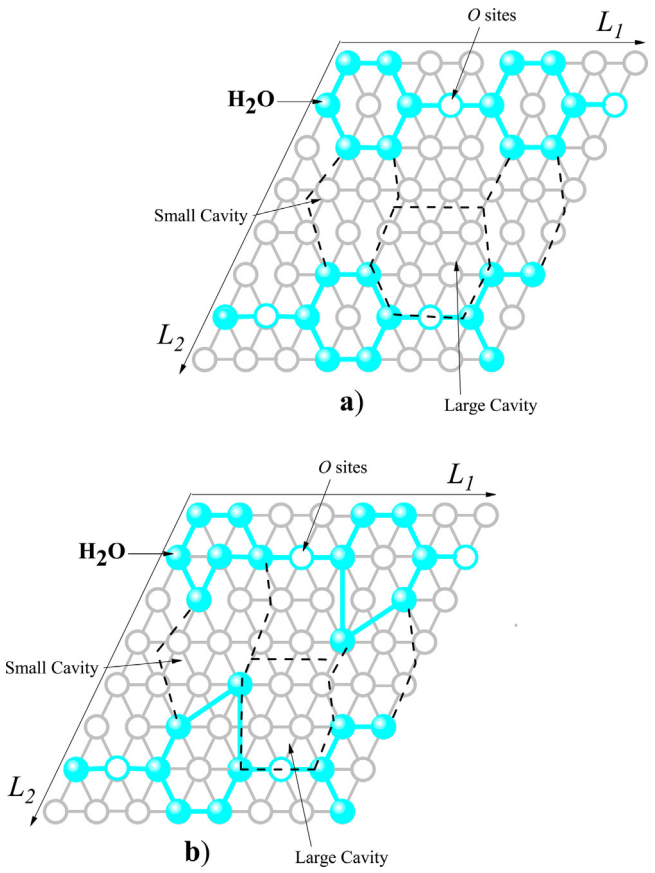

Fig. 2. (a) 2D lattice-gas model for the structure sI of clathrate hydrates. (b) 2D lattice-gas model for the deformed structure sI of clathrate hydrates. Water molecules are represented by previously adsorbed monomers on single sites. Empty sites between the chains of hexagons form the cavities.

Thus, the structure in Fig. 1c can be mimicked by a discrete triangular lattice as shown in Fig. 2. In the figure, occupied sites (cyan circles) represent water molecules and empty sites (empty circles) correspond to small and large cavities. Small cavities are formed by three empty sites and large cavities for five empty sites. As it will be seen in the next section, the guest molecules can be adsorbed on the sites forming the cavities and water molecules can diffuse. However, the water molecules are restricted to return to their original places, in order to keep the original structure the hydrate. Furthermore, the number of monomers is held constant.

Fig. 2 also identifies a specific set of sites, denominated O sites in this work. These are empty sites that appear at the same plane as the hexagons formed by the water molecules. However, they are able to move towards nearest neighbors. These sites should be taken into account as they are closer to water forming the sI plane. Guest molecules near to the O site do not interact energetically. Nevertheless, O site can move due to the strain that can be produced by guest molecules.

2.2. Lattice-gas model: host species or adsorbates

The host species are modeled by a multisite-occupancy adsorption model [45–50]. In this scheme, each guest molecule (CH_4, CO_2) is considered an adsorbate molecule having identical units, and each unit occupying one site on the lattice.

The methane molecule has tetrahedral symmetry with three vertices in its base [52], and accordingly, is represented by the occupancy of three sites (forming a triangle) on the lattice. In the simulation process, the adsorption of a methane molecule is carried out in the following steps: once the first monomer is in its place, the second monomer occupies one of the three NN to the first monomer. As soon as the second neighbor is occupied, the third monomer occupies one of the two closest NN to the first monomer (see Fig. 3a).

In the case of carbon dioxide, the molecule has a linear geometry [52] and is represented by a chain of three consecutive sites: once the first monomer is in its place, the second monomer occupies one of the three NN to the first monomer. Then, the third monomer occupies its NN in the same direction as monomers one and two (see Fig. 3b).

Methane and carbon dioxide molecules have more possible adsorption configurations in large cavities than in small cavities. It is well known that methane molecule is smaller than carbon dioxide molecule [52]. In accordance to Kihara potential parameters [34,53], the core radius of CH_4 molecule is about half the radius of CO_2. These data are consistent with the mapped proportions to the lattice-gas model. As it can be observed from Fig. 3, CO_2 molecule extends (left and right) along a length of three lattice constants, while CH_4 molecule occupies only two sites along the same line.

The model proposed here retains the symmetry of the sI hydrate structure and the relative sizes of the guest molecules. These properties, along with an adequate choice of the lateral interactions, capture the essence of the real systems. The cost of introducing this precursor model is the lack of some experimental features presented by real clathrates. Thus, the relationship between the molecular sizes and the lattice constant is fictitious and has been forced by the discretization of the gas hydrate structure. The development of more sophisticated off-lattice models could contribute to solve this problem.

Finally, the standard Lorentz–Berthelot mixing rules have been used to calculate the potential parameters for the water–guest and guest–guest lateral interactions [34];

$$w_{mn} = \frac{l_{mn}\sqrt{\varepsilon_m \varepsilon_n}}{3} \tag{1}$$

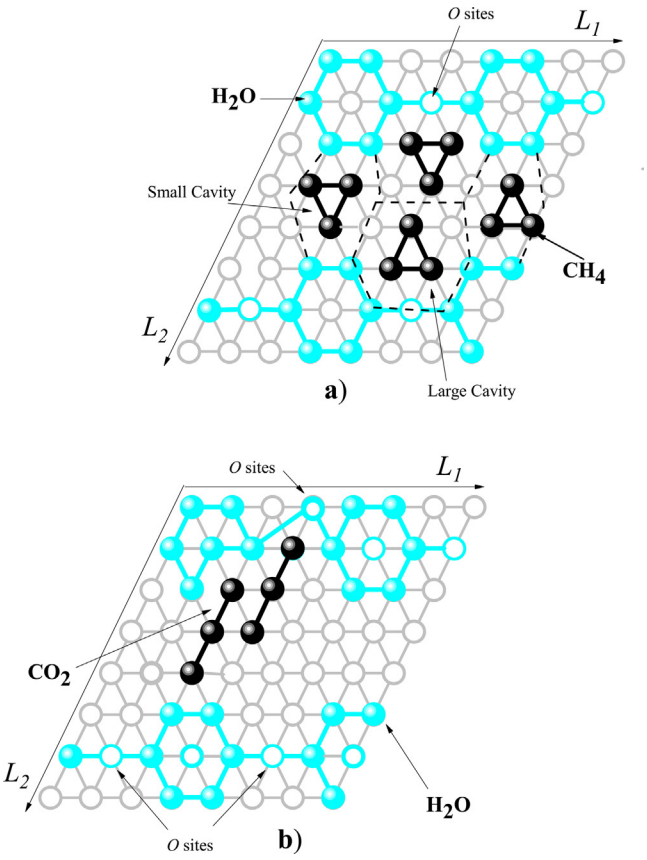

Fig. 3. (a) Guest methane species adsorbed on large and small cavities. (b) Guest carbon dioxide species adsorbed on large and small cavities. Guest molecules of carbon dioxide deform the cavity when they are absorbed.

where l_{mn} is an interaction parameter that can be correlated to experimental data of cavity occupancy. As in Ref. [34], in this work it has been assumed that this interaction parameter is equal to one. ε_m (ε_n) represents the characteristic energy corresponding to the m (n) species. The values of ε_m (ε_n) were taken from Table 2 in Ref. [34]. Interested readers are referred to Ref. [53] for a more complete description of the calculations used to determine ε_m (ε_n). If $m \neq n$, Eq. (1) corresponds to the interaction between different species such as water and methane (H_2O–CH_4) or water and carbon dioxide (H_2O–CO_2). If $m = n$, Eq. (1) represents the interaction between species of the same nature (CH_4–CH_4, CO_2–CO_2 and H_2O–H_2O lateral interactions). Given that w_{mn} represents the site–site lateral interaction, a factor 3 is used in the denominator due to the number of units in the molecule.

2.3. Simulation scheme and thermodynamic quantities

The surface of the hydrate is represented by a matrix of $M = L_1 \times L_2$ sites, where L_1 and L_2 indicate the linear size in the x and y direction, respectively. Water molecules are represented by monomers, which are previously adsorbed. As mentioned in the previous section, the number of monomers is kept constant throughout the adsorption process. Therefore, the total number of available sites for adsorption of guest molecules is $M^* = L_1 \times L_2 - (N_{H_2O} + N_O)$, where $N_{H_2O}$and N_O, represent the number of water molecules and O sites, respectively.

To describe the system of N guest molecules (CH_4 or CO_2) and N_{H_2O} water molecules adsorbed on the lattice at a certain temperature, we introduce the occupation variable c_i. This variable can take the value $c_i = 0$ if the site is empty, $c_i = 1$ if the site is occupied by a guest molecule and $c_i = 2$ if the site is occupied by a water molecule. Guest molecules are absorbed or desorbed as a single unit, avoiding any possible dissociation. Under such considerations, the energy of the system is given by

$$E = \sum_{\langle i,j \rangle} \left[w_{11}\delta_{c_i,1}\delta_{c_j,1} + w_{22}\delta_{c_i,2}\delta_{c_j,2} + w_{1,2}\left(\delta_{c_i,1}\delta_{c_j,2} + \delta_{c_i,2}\delta_{c_j,1}\right)\right] - kNw_{11} \quad (2)$$

where δ is the Kronecker delta function; w_{11} is obtained from Eq. (1) and represents the NN interaction between guest molecules (CH_4–CH_4 or CO_2–CO_2); w_{22} [Eq. (1)] is the NN interaction between water molecules (H_2O–H_2O) and w_{12} [Eq. (1)] corresponds to the NN interaction between a guest molecule and a water molecule (CH_4–H_2O or CO_2–H_2O). w_{11}, w_{12} and w_{22} are considered attractive interactions (w_{11}, w_{12}, $w_{22} < 0$). The pair (i,j) represents all pairs of NN sites. The term kNw_{11} is subtracted in Eq. (2) since the summation over all the pairs of NN sites overestimate the total energy by including kNw_{11} internal bonds belonging to the N adsorbed guest molecules. As it can be seen from Fig. 3, $k = 3$ for CH_4 molecules and $k = 2$ for CO_2 molecules.

In this work, the problem is studied by grand canonical MC (GCMC) simulations using a typical adsorption–desorption algorithm μVT [45–47]. The simulation method consists on performing a number of Monte Carlo steps (MCS), in order to equilibrate the system. After that, mean values of thermodynamic quantities of interest (such as the degree of deformation or the degree of coverage) are obtained as simple averages over successive configurations. Typically, the equilibrium state can be well reproduced after discarding the first $r^* = 10^7$ MCS. Then, the next $r = 2 \times 10^7$ MCS are used to compute averages. This is done for fixed values of temperature T and chemical potential μ (or fugacity in an alternative formulation), while the number N of adsorbed guest molecules can vary.

The algorithm to carry out one MCS is as follows:

1. Set values of chemical potential μ and temperature T.
   a. If the site is empty, an attempt is made to adsorb a guest molecule as described in Section 2.2. The molecule is adsorbed if $\xi < P$, being P the Metropolis probability, $P = \min\{1, \exp[-\beta(\Delta E - \mu\Delta N)]\}$, $\Delta N \rightarrow +1$ [54]. $\beta = 1/k_B T$ (k_B is the Boltzmann constant) and $\Delta E = E_f - E_i$ is the difference between the energies of the final and initial states.
   b. If the site is occupied with a guest molecule, an attempt is made to desorb the molecule as described in Section 2.2. The molecule is desorbed if $\xi < P$, being P the Metropolis probability with $\Delta N = -1$.
   c. If the site is occupied with a H_2O molecule that has not been previously displaced, one of its six NN sites is randomly chosen. If the site is empty, an attempt is made to move the molecule toward the selected site. The molecule is moved if $\xi < P$, being P the Metropolis probability with $\Delta N = 0$.
   d. If the site is occupied with a H_2O molecule that has previously been displaced from its initial position, an attempt is made to return the molecule to the initial configuration. The molecule is moved if $\xi < P$, being P the Metropolis probability with $\Delta N = 0$.
2. Choose randomly one of the M sites, and generate a random number $\xi \in [0,1]$.
3. Repeat from step (2) M times.

In our MC simulations, we varied the chemical potential μ and monitored the density θ and the density of cavities θ_{cavity}, which can be calculated as simple averages:

$$\theta = \frac{3\langle N\rangle}{M*} \text{and} \theta_{\text{cavity}} = \frac{\langle N\rangle}{\text{number of cavities}}, \quad (3)$$

where $\langle \ldots \rangle$ means the average over the r MC simulation runs. Once $\mu(\theta)$ is obtained, the free energy F can be calculated by using the thermodynamic integration method [55]. In the grand canonical ensemble, this method relies on the integration of the chemical potential μ coverage along a reversible path between an arbitrary reference state and the desired state of the system. Thus, for N particles on M^* lattice sites,

$$F(N, M*, T) = F(N_0, M*, T) + \int_{N_0}^{N} \mu dN'. \quad (4)$$

In our case, the determination of the free energy in the reference state, $F(N_0,M^*,T)$, is trivial [$F(N_0,M^*,T) = 0$ for $N_0 = 0$]. Note that the reference state, $N \to 0$, is obtained for $\mu/k_BT \to -\infty$. Then, Eq. (4) can be written in terms of the free energy per site f. Thus,

$$f = \int_0^{\theta} \frac{\mu(\theta')}{3} d\theta'. \quad (5)$$

Finally, the degree of deformation of the lattice D is defined as,

$$D = \frac{\langle N_{\text{mov}}\rangle}{N_{H_2O}+N_O}, \quad (6)$$

where N_{mov} is the number of H_2O molecules and O sites that were displaced from their original locations.

3. Results and discussion

Computer simulations were developed for a 2D lattice-gas model of guest molecules, represented by trimers, and water molecules, represented by monomers, adsorbed on triangular lattices with conventional periodic boundary conditions. As mentioned in previous section, monomers are previously adsorbed and can only diffuse a distance of one lattice constant. The effect of finite size was investigated by examining lattices with $M = L_1 \times L_2 = 40 \times 64$ (768 H_2O molecules and 128 O sites) and $M = L_1 \times L_2 = 80 \times 128$ (3072 H_2O molecules and 512 O sites).

3.1. Degree of deformation

In Section 2.3, the degree of deformation D was defined by Eq. (6). D allows us to obtain information about the distortion of the 2D clathrate hydrate structure, as a consequence of the adsorption of guest molecules in small and large cavities. Using chemical potential μ as a control parameter, θ_{cavity} and D were calculated as simple averages.

In Fig. 4a, the degree of deformation for CH_4 hydrate is shown as a function of θ_{cavity} for different temperatures ranging from 256 K to 298 K. As it has been reported in previous works [24,34], the deformation is associated to the size ratio between cavity and guest molecule. The figure shows the effects of the temperature on the distortion of the structure. Thus, for a fixed value of the lateral interaction, the degree of deformation increases with decreasing temperature. To better understand this behavior, it is more convenient to analyze the curves in terms of the ratio of lateral interactions to temperature (w_{mn}/k_BT). As w_{mn}/k_BT is increased (decreasing values of T), lateral couplings between host–host and host–water are important and strongly affect (distort) the hydrate structure.

For all temperatures, the curves of D vs θ_{cavity} decrease with the filling of the cavities and reach a minimum value when the structure sI has one molecule per cavity, i.e, $\theta_{\text{cavity}} \approx 1$.

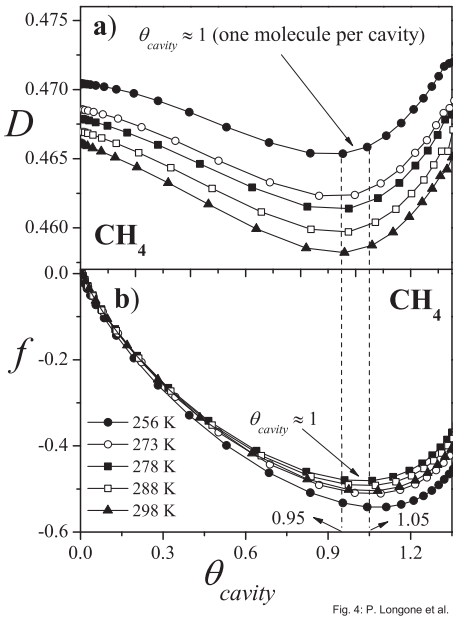

Fig. 4. (a) Degree of deformation D and (b) free energy per site f (in units of β) as a function of the coverage of the cavities θ_{cavity} for CH_4 hydrates. The curves correspond MC simulations for $L_1 = 80$, $L_2 = 128$ and different temperatures as indicated.

Curves in Fig. 4b show the behavior of the free energy per site f for the cases reported in Fig. 4a, calculated according to the procedure described in Section 2.3. f shows a minimum around $\theta_{\text{cavity}} \approx 1$ (between 0.95 and 1.05). This means that the range of the minimum deformation coincides with the range of the minimum free energy. This important result demonstrates that the most stable state of the system occurs when one methane molecule is adsorbed per cavity. From this minimum, an increase in the chemical potential leads to more than one adsorbed molecule per cavity and, consequently, causes an increase in D. Above $\theta_{\text{cavity}} \approx 1$, the free energy per site increases and the hydrate loses stability. For $\theta_{\text{cavity}} = 0$, the 2D hydrate structure is empty (initially is considered stable structure) and the interaction is only between the H_2O–H_2O molecules. In this case, it is clearly seen how D is affected by the relationship between temperature and lateral interactions. Curves at higher temperatures have lower values of the degree of deformation D.

The study in Fig. 4 was repeated for carbon dioxide molecules. The results are shown in Fig. 5. CO_2 is a larger molecule than methane, and this difference is reflected in the behavior of the deformation. In this case, the curves of D vs θ_{cavity} increase with the filling of the cavities, pass by a maximum and go to a minimum for $\theta_{\text{cavity}} \approx 1$. For $\theta_{\text{cavity}} > 1$, the deformation increases sharply. In contrast to CH_4 hydrate, the minimum value of the degree of deformation for CO_2 hydrate does not match with the minimum value of the free energy per site. As it can be observed in Fig. 5b, f decreases with coverage and passes through a minimum at $\theta_{\text{cavity}} \approx 1.35$. From this value of coverage, the free energy per site increases.

Despite the behavior of the free energy per site, it is assumed here that the minimum of deformation is the most stable condition for CO_2 hydrate. The condition of one molecule per cavity has been considered for different author in calculating stability points and developing phase diagrams [16,17,31,34]. The observed shift in the f curves can be attributed to simplifications made in the model. In fact, CO_2 guest molecules have preference for large cavities [1,56–59] and this preference has not been considered in our model.

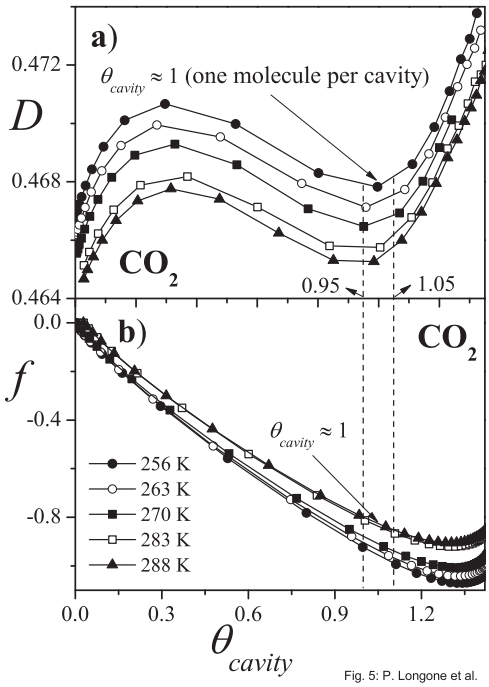

Fig. 5. Same as Fig. 4 for CO_2 hydrates.

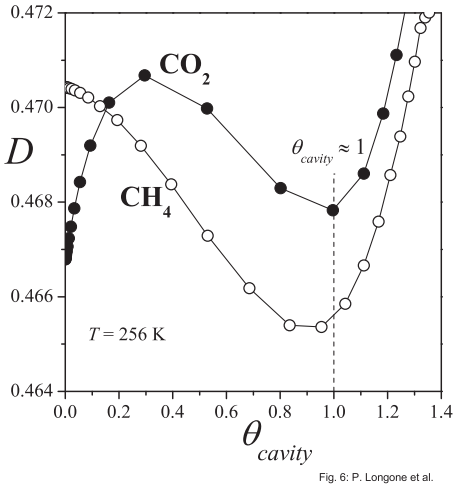

Fig. 6. Degree of deformation versus θ_{cavity} for CO_2 and CH_4 hydrates.

Fig. 6 presents the degree of deformation D as a function of θ_{cavity} for CH_4 and CO_2 hydrates at the same temperature. It can be seen that CO_2 molecules produce a greater deformation than CH_4 molecules because CO_2 molecules are larger than CH_4 molecules. Furthermore, both host species show a minimum deformation at $\theta_{cavity} \approx 1$.

3.2. Stability phase diagram

According to the results presented in the previous section, the stability phase diagram for each host species is constructed considering the minimum value of D and its corresponding chemical potential $\beta\mu$ (in units of β). As the present study was performed in the grand canonical assembly μVT, the results are given in terms of chemical potential instead of pressure. In addition, and due to the simplifications introduced in the system, the control parameter used here is a pseudo-chemical potential and is not directly associated with the standard chemical potential $\beta\mu = \ln(\Lambda^3\rho)$, where Λ is the de Broglie wavelength and ρ is the molar density [38]. In the rest of the paper, we will denote this pseudo-chemical potential by μ^*.

Fig. 7a shows the $(\beta\mu^* - T)$ phase diagram for CH_4 species in the temperature range 255–320 K. The blue dots are obtained from the values of the minima in Fig. 4a. Blue dashed line, obtained by linking the blue dots, represents the phase diagram for the 2D sI structure of the CH_4 hydrate. For low temperatures (in the range 255–273 K), $\beta\mu^*$ increases linearly with T. A change in the shape of the curve is observed at 273 K. This point is qualitatively similar to the quadruple point reported in Ref. [60]. For temperatures in the range 273–320 K, $\beta\mu^*$ has an exponential increase with T.

Even though the values of the chemical potentials obtained here do not quantitatively correspond to those reported in the literature, the phase diagram of Fig. 7a is in qualitative agreement with theoretical [2,60] and experimental [61] phase diagrams reported in literature. However, the blue line is not a coexistence line of a binary system (water + methane) as other authors showed [2,60]. Instead, blue line defines a region of stability for methane hydrate. Above the blue line, methane hydrate is in its most stable state, i.e. each cavity is occupied by a molecule of methane. This phenomenon allows the formation and stabilization of the structure sI 2D because of the lattice distortion is at its minimum. Below the blue line, methane hydrate is unstable (the excess of guest molecules leads to an increase in the deformation of the sI structure). A similar behavior has been observed by Sizov and Petrovskaya [26], by using Monte Carlo simulation for a 3D flexible lattice model. The authors modeled water through SPC/E model [35] and methane by united-atom (UA) Lennard-Jones model [36]. They proved that the presence of more than one methane molecule in each cavity produces a deformation of the sI structure. One molecule per cavity preserves the shape and, therefore, the stability of the hydrate.

On the other hand, for the case of CO_2 hydrates, the corresponding phase diagram is shown in Fig. 7b. In the temperature range between 255 K and 265 K, $\beta\mu^*$ is constant with increasing T. At 265 K, $\beta\mu^*$ begins to increase exponentially

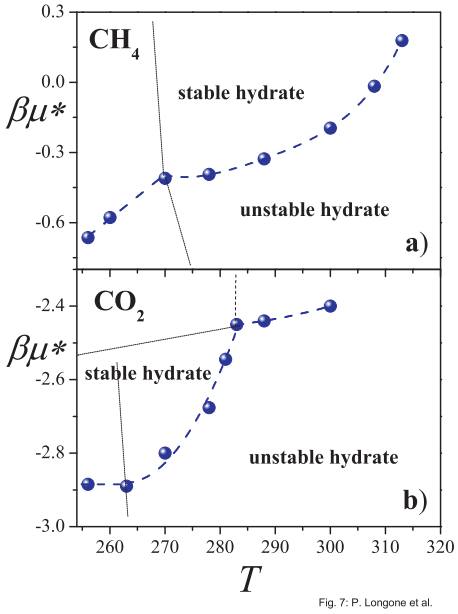

Fig. 7. $(\mu^* - T)$ phase diagrams for CH_4 [part (a)] and CO_2 [part (b)] hydrates. Above the blue dashed line CH_4 (CO_2) hydrate is in its most stable state and below the blue dashed line CH_4 (CO_2) hydrate is unstable. The blue dashed lines are not coexistence lines. However, the curves are in qualitative agreement with phase diagrams reported in Refs. 60–62]. (For interpretation of the references to color in this figure legend, the reader is referred to the web version of this article.)

with T until a temperature of 283 K. For high temperatures (in the range 283–300 K), a moderate increase is observed in the curve of $\beta\mu^*$ vs T. Abrupt changes in the slope of the curve are observed at 263 and 283 K. A qualitatively similar behavior has been reported in the literature [60,62]. This qualitative agreement is remarkable. However, as mentioned above, the CO_2 and CH_4 hydrate equilibrium predictions derived in this paper are not directly comparable with experimental data, due to the fictitious molecular size/geometry of the gases and the use of an equivalent pseudo chemical potential instead of the exact chemical potential at the specified conditions.

4. Conclusions

In this work, a 2D lattice-gas model and MC simulations have been used to study the stability and degree of deformation of sI gas hydrates the presence of CH_4 and CO_2 species. The results reported represent stability points (or minimal deformation) of the 2D sI structure in the presence of adsorbed host species (CH_4 and CO_2), and they are not a correlation of theoretical and experimental phase equilibrium data. According to the present analysis, the behavior of the system is characterized by the following properties:

1. Taking into account the interaction energies, the degree of deformation for the sI structure decreases with increasing temperature. Species–species and species–water lateral interactions prevail at low temperatures. This behavior is observed for both methane and carbon dioxide hydrates.
2. For methane hydrates, the degree of deformation first decreases, then reaches a minimum value and finally rises with the adsorption of host species in large and small cavities. The minimum deformation is found at coverage close to one, when a molecule is adsorbed per cavity. This condition matches the minimum value of the free energy (most stable state) of the system.
3. In the case of carbon dioxide hydrates, the degree of deformation first increases, passes by a maximum and then reaches a minimum value and finally rises with the adsorption of host species in large and small cavities. The minimum deformation is also found at coverage close to one, but this density does not correspond with the minimum of the free energy. This is because carbon dioxide has a preference for larger cavities, and only low CO_2 occupancies are found in small cavities. However, in this work the minimum deformation is considered as the most stable state for the system.
4. ($\mu^* - T$) phase diagrams were calculated with the corresponding values of the chemical potential at the minimum deformation. These phase diagrams are in qualitative agreement with those reported in the literature for both methane and carbon dioxide. Lines in phase diagrams are not phase coexistence lines, but they delimit the stability and non-stability regions of the gas hydrates.

Acknowledgments

This work was supported in part by CONICET (Argentina) under project PIP112-201101-00615; Universidad Nacional de San Luis (Argentina) under project 322000; and the National Agency of Scientific and Technological Promotion (Argentina) under project PICT-2013-1678.

References

[1] E.D. Sloan, Fundamental principles and applications of gas hydrates, Nature 426 (2003) 353–359.
[2] E.D. Sloan, C.A. Khoh, Clathrate Hydrates of Natural Gases, third ed., CRC Press, Boca Raton, FL, USA, 2007.
[3] G.A. Jeffrey, in: J.L. Atwood, J.E.D. Davies, D.D. McNicol (Eds.), Inclusion Compounds, 1, Academic Press, London, 1984 p. 135.
[4] G.A. Jeffrey, R.K. McMullan, The clathrate hydrates, Prog. Inorg. Chem. 8 (1967) 43–108.
[5] T.S. Collett, Energy resource potential of natural gas hydrates, AAPG Bull. 86 (2002) 1971–1992.
[6] M.R. Walsh, S.H. Hancock, S. Wilson, S.L. Patil, G.J. Moridis, R. Boswell, T.S. Collett, C.A. Koh, E.D. Sloan, Preliminary report on the commercial viability of gas production from natural gas hydrates, Energy Econ. 31 (2009) 815–823.
[7] G.J. Moridis, T.S. Collett, R. Boswell, M. Kurihara, M.T. Reagan, C. Koh, E.D. Sloan, Towards production from gas hydrates: current status, assessment of resources, and simulation based evaluation of technology and potential, SPE Reservoir Eval. Eng. 12 (2009) 745–771.
[8] K.A. Kvenvolden, A review of the geochemistry of methane in natural gas hydrate, Org. Geochem. 23 (1995) 997–1008.
[9] J.B. Klauda, S.I. Sandler, Global distribution of methane hydrate in ocean sediment, Energy Fuels 19 (2005) 459–470.
[10] (a) S. Wroblewski, On the combination of carbonic acid and water, Acad. Sci. Paris C. R. 9 (1882) 212–213;
(b) M.P. Villard, Experimental study of gas hydrates, Ann. Chim. Phys. 11 (7) (1897) 353–360.
[11] K. Kvenvolden, Potential effects of gas hydrate on human welfare, Proc. Natl. Acad. Sci. U. S. A. 96 (1999) 3420–3426.
[12] K. Kvenvolden, Gas hydrate and humans, Ann. N. Y. Acad. Sci. 912 (2000) 17–22.
[13] S.G. Hatzikiriakos, P. Englezos, On the Relationship between global warming and methane gas hydrates in the earth, Chem. Eng. Sci. 48 (1993) 3963–3969.
[14] K.A. Kvenvolden, G. Claypool, Gas hydrates in oceanic sediment U.S. Geological Survey Open File Report 50, Dept. of the Interior, U.S. Geological Survey, Denver, Colo. (1988) 88–216.
[15] P.G. Brewer, G. Friederich, E.T. Peltzer, F.M. Orr, Direct experiment on the ocean disposal of fossil fuel CO_2, Science 284 (1999) 943–945.
[16] J.H. van der Waals, J.C. Platteeuw, Clathrate solutions, Adv. Chem. Phys. 2 (1959) 1–57.
[17] W.R. Parrish, J.M. Prausnitz, Dissociation pressures of gas hydrates formed for by gas mixtures, Ind. Eng. Chem. Process Des. Dev. 11 (1972) 26–34.
[18] H. Tanaka, The thermodynamic stability of clathrate hydrate. III. Accommodation of nonspherical propane and ethane molecules, J. Chem. Phys. 101 (1994) 10833–10842.
[19] R.E. Westacott, M.P. Rodger, Full-coordinate free-energy minimisation for complex molecular crystals: type I hydrates, Chem. Phys. Lett. 262 (1996) 47–51.
[20] H. Tanaka, T. Nakatsuka, K. Koga, On the thermodynamic stability of clathrate hydrates IV: double occupancy of cages, J. Chem. Phys. 121 (2004) 5488–5493.
[21] A.A. Chialvo, M. Houssa, P.T. Cummings, Molecular dynamics study of the structure and thermophysical properties of model sI clathrate hydrates, J. Phys. Chem. B 106 (2002) 442–451.
[22] P.M. Rodger, Stability of gas hydrates, J. Phys. Chem. 94 (1990) 6080–6089.
[23] P.M. Rodger, Lattice relaxation in type I gas hydrates, AIChE J. 37 (1991) 1511–1516.
[24] S.R. Zele, S.-Y. Lee, G.D. Holder, A theory of lattice distortion in gas hydrates, J. Phys. Chem. B 103 (1999) 10250–10257.
[25] S.J. Wierzchowski, P.A. Monson, Calculation of free energies and chemical potentials for gas hydrates using Monte Carlo simulations, J. Phys. Chem. B 111 (2007) 7274–7282.
[26] V. Vladimir Sizov, M. Elena Piotrovskaya, Computer simulation of methane hydrate cage occupancy, J. Phys. Chem. B 111 (2007) 2886–2890.
[27] N.I. Papadimitriou, I.N. Tsimpanogiannis, A. Th Papaioannou, A.K. Stubos, Evaluation of the hydrogen-storage capacity of pure H_2 and binary H_2-THF hydrates with Monte Carlo simulations, J. Phys. Chem. C 112 (2008) 10294–10302.
[28] N.I. Papadimitriou, I.N. Tsimpanogiannis, A.K. Stubos, Computational approach to study hydrogen storage in clathrate hydrates, Colloids Surf. A 357 (2010) 67–73.
[29] I.N. Papadimitriou, Monte Carlo study of sI hydrogen hydrates, Mol. Simul. 36 (2010) 736–744.
[30] N.I. Papadimitriou, I.N. Tsimpanogiannis, A.K. Stubos, Monte Carlo simulations of methane hydrates, Proceedings of the 7th International Conference on Gas Hydrates (ICGH 2011), Edinburgh, Scotland, United Kingdom, 2011, pp. 17–21.
[31] H. Pimpalgaonkar, S.K. Veesam, S.N. Punnathanam, Theory of gas hydrates: effect of the approximation of rigid water lattice, J. Phys. Chem. B 115 (2011) 10018–10026.
[32] N.I. Papadimitriou, I.N. Tsimpanogiannis, A.K. Stubos, A. Martín, L.J. Rovetto, L.J. Florusse, C.J. Peters, Experimental and computational investigation of the sII binary He-THF hydrate, J. Phys. Chem. B 115 (2011) 1411–1415.
[33] O. Teleman, B. Jönsson, Vectorizing a general purpose molecular dynamics simulation program, J. Comput. Chem. 7 (1986) 58–66.
[34] A. Martín, C.J. Peters, New thermodynamic model of equilibrium states of gas hydrates considering lattice distortion, J. Phys. Chem. C 113 (2009) 422–430.
[35] H.J.C. Berendsen, J.R. Grigera, T.P. Straatsma, The missing term in effective pair potentials, J. Phys. Chem. 91 (1987) 6269–6271.
[36] W.L. Jorgensen, J.D. Madura, C.J. Swenson, Optimized intermolecular potential functions for liquid hydrocarbons, J. Am. Chem. Soc. 106 (1984) 6638–6646.
[37] D.A. Lavis, Equilibrium Statistical Mechanics of Lattice Models, Springer, London, 2015.

[38] T.L. Hill, An Introduction to Statistical Thermodynamics, Addison Wesley, Reading, MA, 1960.
[39] K.G. Wilson, The renormalization group: critical phenomena and the Kondo problem, Rev. Mod. Phys. 47 (1975) 773–840.
[40] R.J. Baxter, Exactly Solved Models in Statistical Mechanics, Academic Press, New York, 1982.
[41] V. Privman, Finite-Size Scaling and Numerical Simulation of Statistical Systems, World Scientific, Singapore, 1990.
[42] W. Lenz, Beiträge zum Verständnis der magnetischen Eigenschaften in festen Körpern, Phys. Z. 21 (1920) 613–615.
[43] E. Ising, Beitrag zur Theorie des Ferromagnetismus, Z. Phys. 31 (1925) 253–258.
[44] L. Onsager, Crystal statistics. I. A two-dimensional model with an order-disorder transition, Phys. Rev. 65 (1944) 117–149.
[45] J.E. González, A.J. Ramirez-Pastor, V.D. Pereyra, Adsorption of dimer molecules on triangular and honeycomb lattices, Langmuir 17 (2001) 6974–6980.
[46] F. Romá, J.L. Riccardo, A.J. Ramirez-Pastor, Statistical thermodynamics models for polyatomic adsorbates: application to adsorption of *n*-paraffins in 5A zeolite, Langmuir 21 (2005) 2454–2459.
[47] M. Dávila, F. Romá, J.L. Riccardo, A.J. Ramirez-Pastor, Quasi-chemical approximation for polyatomics: statistical thermodynamics of adsorption, Surf. Sci. 600 (2006) 2011–2025.
[48] F. Romá, J.L. Riccardo, A.J. Ramirez-Pastor, Application of the fractional statistical theory of adsorption (FSTA) to adsorption of linear and flexible k-mers on two-dimensional surfaces, Ind. Eng. Chem. Res. 45 (2006) 2046–2053.
[49] A.J. Ramirez-Pastor, M.S. Nazzarro, J.L. Riccardo, G. Zgrablich, Dimer physisorption on heterogeneous substrates, Surf. Sci. 341 (1995) 249–261.
[50] M.C. Giménez, A.J. Ramirez-Pastor, E.P.M. Leiva, Monte Carlo simulation of metal deposition on foreign substrates, Surf. Sci. 600 (2006) 4741–4751.
[51] M. Chaplin, Water structure and science, [on-line]. This work is licensed under a Creative Commons Attribution-Noncommercial-No Derivative Works 2.0 UK: England & Wales License. G. Crane, Editor-in-Chief. <http://www1.lsbu.ac.uk/water/clathrat2.html#si>, 2003 (consultation August 2012).
[52] R.T. Morrison, R.N. Boyd, Organic Chemistry, Prentice-Hall International, New Jersey, 1992.
[53] L.S. Tee, S. Gotoh, W.E. Stewart, Molecular parameters for normal fluids: the kihara potential with spherical core, Ind. Eng. Chem. Fund. 5 (1966) 363–367.
[54] N. Metropolis, A.W. Rosenbluth, M.N. Rosenbluth, A.H. Teller, E. Teller, Equation of state calculations by fast computing machines, J. Chem. Phys. 21 (1953) 1087–1092.
[55] K. Binder, Static and dynamic critical phenomena of the two-dimensional q-state Potts model, J. Stat. Phys. 24 (1981) 69–86 and references therein.
[56] A. Khan, Theoretical studies of $CO_2(H_2O)_{20,24,28}$ clusters: stabilization of cages in hydrates by CO_2 guest molecules, J. Mol. Struct. (THEOCHEM) 664–665 (2003) 237–245.
[57] K.A. Udachin, C.I. Ratcliffe, J.A. Ripmeester, Structure, composition, and thermal expansion of CO_2 hydrate from single crystal X-ray diffraction measurements, J. Phys. Chem. B 105 (2001) 4200–4204.
[58] J.A. Ripmeester, J.S. Tse, C.I. Ratcliffe, B.M. Powell, Nature 135 (325) (1987) .
[59] J.A. Ripmeester, C.I. Ratcliffe, Xenon-129 NMR studies of clathrate hydrates: new guests for structure II and structure H, J. Phys. Chem. 94 (1990) 8773–8776.
[60] Y. He, E.S.J. Rudolph, P.L.J. Zitha, M. Golombok, Kinetics of CO_2 and methane hydrate formation: an experimental analysis in the bulk phase, Fuel 90 (2011) 272–279.
[61] J.M. Schicks, Gas hydrates, Annu. Rep. Prog. Chem. Sect. C: Phys. Chem. 106 (2010) 101–117.
[62] S.O. Yang, I.M. Yang, Y.S. Kim, C.S. Lee, Measurement and prediction of phase equilibria for water + CO_2 in hydrate forming conditions, Fluid Phase Equilib. 175 (2000) 75–89.